Glassy systems under time-dependent driving forces: Application to slow granular rheology

L. Berthier,[1] L. F. Cugliandolo,[2] and J. L. Iguain[3],*

[1]*Laboratoire de Physique, École Normale Supérieure de Lyon, 46 Allée d'Italie, F-69007 Lyon, France*
and Département de Physique des Matériaux, UCB Lyon 1, 69622 Villeurbanne Cedex, France
[2]*Laboratoire de Physique Théorique, École Normale Supérieure, 24 rue Lhomond, F-75231 Paris Cédex 05, France*
and Laboratoire de Physique Théorique et Hautes Énergies, Jussieu, 4 Place Jussieu, F-75252 Paris Cédex 05, France
[3]*Departamento de Física, Universidad Nacional de Mar del Plata, Deán Funes 3350, 7600 Mar del Plata, Argentina*
(Received 19 October 2000; published 12 April 2001)

We study the dynamics of a glassy model with infinite range interactions externally driven by an oscillatory force. We find a well-defined transition in the (temperature-amplitude-frequency) phase diagram between (i) a ''glassy'' state characterized by the slow relaxation of one-time quantities, aging in two-time quantities and a modification of the equilibrium fluctuation-dissipation relation; and (ii) a ''liquid'' state with a finite relaxation time. In the glassy phase, the degrees of freedom governing the slow relaxation are thermalized to an effective temperature. Using Monte Carlo simulations, we investigate the effect of trapping regions in phase space on the driven dynamics. We find that it alternates between periods of rapid motion and periods of trapping. These results confirm the strong analogies between the slow granular rheology and the dynamics of glasses. They also provide a theoretical underpinning to earlier attempts to present a thermodynamic description of moderately driven granular materials.

I. INTRODUCTION

In recent years, granular matter has received growing attention from the physics community [1]. The study of powders is relevant not only because granular materials have many industrial applications but also because it raises many fundamental questions of physical interest.

We call granular matter all many-body systems constituted by grains of macroscopic size. The grains interact via repulsive dissipative forces due to inelastic collisions and static friction. The thermal energy scale is totally negligible with respect to the typical gravitational energy. In the absence of external perturbations, each metastable configuration has an infinite lifetime, and thermal averaging is meaningless. The static properties of such systems are hence very interesting, the sandpile problem being the paradigm [1].

Powders flow only when energy is supplied externally. This can be done by applying a shear or a vibration. The dynamics of granular matter presents a very rich phenomenology that depends not only on the intensity of the drive, generically called Γ, but also on the way the granular system is driven [1]. A weak driving force can be provided by applying ''taps'' to the systems, as has been done in the pioneering experiments of the Chicago group [2], where the parameter Γ is the reduced acceleration of the taps. Recently, Nicolas *et al.* investigated the dynamics of a powder by sinusoidally shearing it in a weak manner [3]; Γ here is the maximal amplitude of the strain. Experiments reveal that the time evolution, in the gently driven situation, is characterized by an extremely slow dynamics [2–4]. In the tapping experiments for instance, the density still evolves after 10^5 taps [2]. When the energy injection is much stronger, the granular matter eventually becomes fluid; it behaves essentially like a

dissipative gas, and is described by a hydrodynamic theory that takes into account energy dissipation through the collisions between the grains [1,5]. In this work we shall focus on the gently driven regime, and we shall not address the strongly perturbed situation.

This phenomenology is clearly reminiscent of the behavior of glass forming systems, for which the control parameter is the temperature T (or the density ρ) [6–10]. At high T (say), the samples are in the liquid or gaseous phases. When T decreases, their dynamics becomes exceedingly slow, and may even appear to stop completely during the experimental time window. However, at temperatures above but close to the glass transition, the relaxation reaches a stationary regime characterized by the decay of all correlations in two steps, the second decay being related to the structural relaxation. At temperatures below the glass transition temperature, the structural relaxation time t_r depends on the time spent in the glassy phase (the ''waiting time'' t_w, or ''age''), and typically $t_r \propto t_w$ [11]. A stationary regime cannot be reached experimentally. This is the aging effect which has been observed in a wide spectrum of glassy systems such as plastics [12], spin glasses [13], glycerol [14], dielectric glasses [15], complex fluids [16], phase separating systems [17], etc.

Recently, the similitude in the dynamics of granular matter under vibration and glass forming materials was rationalized by Liu and Nagel [7]. These authors proposed a phase diagram that unifies the physics of glassy systems and granular materials. In its simplest version, the diagram has three axes (T, ρ, Γ). The (T, ρ) plane describes the physics of glasses, while the (ρ, Γ) plane describes the one of athermal driven systems, like powders or foams. In the low-T, high-ρ, small-Γ region, the system is generically jammed or presents glassy features. In this work, we focus on the (Γ, T) plane of this phase diagram. The drive axis Γ can represent two types of forces: (1) ''shearlike'' forces that do not derive

*Present address: LPTHE, 4 Place Jussieu, F-75252 Paris Cedex 05, France.

from a potential and hence do work on the sample [18]; and (2) ''tappinglike'' forces that do derive from a potential but work on the samples when they depend on time. Both modify the dynamic behavior, and the goal is to identify how, and to what extent, in a general manner. One possible scenario is that the age of the driven system stabilizes at a power dependent level, typically $t_r \propto \Gamma^{-1}$. In rheological language, this is a shear-thinning behavior. Some examples are given by domain growth under flow [19] or by the nonlinear rheology of complex fluids [20], and it has been captured by a number of models [21–23]. In particular, a (shear, temperature) phase diagram for glassy systems was derived in Ref. [21]. Another scenario, realized in the present paper, is that aging is not stopped, at least in a well-delimited region of the phase diagram.

The behavior of moderately driven granular matter has received a lot of experimental [2–4,24,25], numerical [9,26–29] and theoretical [8,10,30–38] attention. All these studies demonstrated the glassy nature of granular compaction below a critical amplitude of the drive, $\Gamma^\star$. This was first revealed by the very slow relaxation of the density, but memory experiments [24] and simulations [28,31] inspired by earlier spin glass studies [11,13] also gave support to this conclusion.

The relation between granular matter and glassy systems is widely assumed. Indeed, many of the models proposed to study granular compaction are directly adapted from glassy models [8,26–29,36–38]. Usually, the drive Γ in granular matter is related to the temperature T in glasses. However, the assumed relationship $T = T(\Gamma)$ between the drive and the temperature is a highly nontrivial statement and there is, to our knowledge, no microscopic approach that justifies this. *We do not make such an assumption here.* In this respect, Mehta *et al.* [8] built a phenomenological two-temperature stochastic model based on the observation that slow granular compaction is basically a two-step process: in this model, a short-time process stands for fast independent-particle relaxation, while a slow one stands for cooperative rearrangements. The recent experiment of Nicolas *et al.* [3] clearly proved the existence of these two (uncorrelated) processes. A two-step process, each step thermalized with its own temperature, is precisely the output of previous studies of the constantly driven dynamics of glassy systems in a thermal bath [18,21], confirmed by the numerical simulation of a sheared supercooled liquid [39].

In this paper we study the dynamics of a glassy system permanently perturbed by a time-dependent Hamiltonian force [40–42]. Our aim is to identify which properties correspond to those observed experimentally in granular systems, and whether an effective temperature for the slow degrees of freedom is generated in this weakly athermal system. In some sense, our approach is ''orthogonal'' to previous ones. We do not propose a new model for the slow granular rheology, but rather ask the following simpler question: *What is the behavior of a glassy system subjected to periodic driving forces?* To answer this question, the (T, Γ, ω) phase diagram is explored. This is done by studying the dynamics of the, by now standard, mean-field glass model, the p-spin glass model [11,43,44], under a time-dependent

driving force. (Despite its name, that follows from historical reasons, this model represents a structural glass and not a spin glass.) We then discuss how our results have to be interpreted in the context of granular materials.

The paper is organized as follows. In Sec. II, we recall the definition and main properties of the p-spin glass model. Its behavior under an oscillatory drive, for the choice of parameters $p=2$ and $p \geq 3$, is examined in Secs. III and IV, respectively, in two ways: analytical and numerical solutions of the spherical model, and Monte Carlo simulations of the Ising model. We discuss our results in the context of slow granular rheology in Sec. V. Our conclusions close the paper in Sec. VI.

II. DEFINITION AND ZERO-DRIVE BEHAVIOR OF THE MODEL

The spherical p-spin glass, when $p=2$, is simply the spherical version of the Sherrington-Kirkpatrick spin glass, and was introduced by Kosterlitz *et al.* [45] as an exactly solvable model. It is in fact equivalent to the $O(n)$, $n \to \infty$, model for ferromagnetic domain growth in three dimensions. Its statics [45] and its relaxational dynamics have been extensively studied [46–48]. The $p \geq 3$ spherical models are instead simplified models for supercooled liquids and glasses, in the sense that they give a theoretical framework to understand both the statics [11,43,49] and the nonequilibrium dynamics [11,50] of glass forming systems. We study these two cases as generic glassy models, taking advantage of the fact that exact equations for their driven dynamics can be derived.

A. Model

The p-spin glass model in its spherical [44] and Ising [43,51] versions is defined by the Hamiltonian

$$H_J[\mathbf{s}] = \sum_{i_1 < i_2 < \ldots < i_p} J_{i_1 i_2 \ldots i_p} s_{i_1} s_{i_2} \ldots s_{i_p}, \qquad (1)$$

where the couplings $J_{i_1 i_2 \ldots i_p}$ are random Gaussian variables with zero mean and variance $\overline{(J_{i_1 i_2 \ldots i_p})^2} = p!/(2N^{p-1})$. The spins $\{s_i, i=1, \ldots, N\}$ may satisfy a global spherical constraint $\Sigma_i s_i^2(t) = N$, or be Ising variables $s_i = \pm 1$. In the spherical version, the driven dynamics is given by the Langevin equation

$$\frac{\partial s_i(t)}{\partial t} = -\frac{\delta H}{\delta s_i(t)} - z(t) s_i(t) + f_i^{\text{TAPPING}}(t) + \eta_i(t), \quad (2)$$

where the parameter $z(t)$ ensures the spherical constraint, and $\eta_i(t)$ is the thermal noise, taken from a Gaussian distribution with zero mean and variance $2k_B T$. [In what follows we use units such that the Boltzmann constant k_B is 1.] The thermal bath temperature T can possibly be zero. In the Ising version one can still write down a continuous Langevin equation by using soft spins and taking the Ising limit at the end of the calculations. The spherical version is simpler to

treat analytically, while the Ising version is much simpler to deal with using Monte Carlo simulations, since the spins are bimodal variables.

In order to mimic tapping experiments, a periodic time-dependent Hamiltonian force $f_i^{\mathrm{TAPPING}}(t)$ has to be added to the right hand side of the Langevin equation (2). The simplest periodic time dependence one can think of is a cosine form of period $\tau \equiv 2\pi/\omega$. Thus we are led to add a magnetic field in Hamiltonian (1):

$$H_J[\mathbf{s}] \to H_J[\mathbf{s}] + \cos(\omega t) \sum_{i=1}^{N} h_i s_i(t). \qquad (3)$$

In the most realistic numerical experiments, the tapping is modeled by a two-step dilation-relaxation process [9], while, in more schematic models, the driving force is not explicitly time dependent [26,28,29,31]. Two types of spatial dependence of the field will be considered below: constant, $h_i = h$, for all sites i, and random, $\overline{h_i h_j} = h^2 \delta_{ij}$. There are, however, no physical differences between the two situations, since a spatially constant field is as decorrelated from the ground states of the Hamiltonian $H_J[\mathbf{s}]$ as a random one.

B. Dynamical equations

The dynamics of the spherical version of the model is better analyzed in terms of the autocorrelation function $C(t,t') \equiv \sum_i \overline{\langle s_i(t) s_i(t') \rangle}/N$ and the linear response function $R(t,t') \equiv \sum_i \overline{\langle s_i(t) \eta_i(t') \rangle}/(2TN)$ since, in the thermodynamic limit $N \to \infty$, C and R verify closed Schwinger-Dyson equations which read, for $t > t'$ [50],

$$\frac{\partial C(t,t')}{\partial t} = -z(t) C(t,t')$$

$$+ \frac{p(p-1)}{2} \int_0^t dt'' C^{p-2}(t,t'') R(t,t'') C(t'',t')$$

$$+ \frac{p}{2} \int_0^{t'} dt'' C^{p-1}(t,t'') R(t',t'')$$

$$+ h^2 \cos(\omega t) \int_0^{t'} dt'' \cos(\omega t'') R(t',t''),$$

$$\tag{4}$$

$$\frac{\partial R(t,t')}{\partial t} = -z(t) R(t,t')$$

$$+ \frac{p(p-1)}{2} \int_{t'}^t dt'' C^{p-2}(t,t'') R(t,t'') R(t'',t'),$$

$$z(t) = T + \frac{p^2}{2} \int_0^t dt'' C^{p-1}(t,t'') R(t,t'')$$

$$+ h^2 \cos(\omega t) \int_0^t dt'' \cos(\omega t'') R(t,t'').$$

These integrodifferential equations are complemented by the equal-time conditions $C(t,t) = 1$ and $R(t^+,t) = 1$, the sym-

metry of the correlation, $C(t,t') = C(t',t)$, and the causality $R(t',t) = 0$. In deriving these equations, a random initial condition at time $t = 0$ has been used, which can be interpreted as an equilibrium configuration at infinite temperature. An infinitely fast quench toward the final temperature T is performed at $t = 0$, and the evolution continues at subsequent times in isothermal conditions. The energy density $e(t) \equiv N^{-1} \langle \overline{H_J[\mathbf{s}]} \rangle$ is related to the constraint $z(t)$ through

$$e(t) = \frac{1}{p}[T - z(t)]. \qquad (5)$$

In Eqs. (4), the oscillatory field has been chosen to be constant in space.

In the $p = 2$ case, the dynamics simplifies considerably since it can be solved directly from the Langevin equation (2). Indeed, this set of N differential equations is diagonalized by using the basis of eigenvectors of the symmetric matrix J_{ij}. Denoting $\boldsymbol{\mu}$ the eigenvector associated with the eigenvalue μ, and $s_\mu \equiv \boldsymbol{\mu} \cdot \mathbf{s}$ and $h_\mu \equiv \boldsymbol{\mu} \cdot \mathbf{h}$ the projections of the spin and field onto the eigenvectors, one obtains

$$\frac{\partial s_\mu(t)}{\partial t} = [\mu - z(t)] s_\mu(t) + h_\mu \cos(\omega t) + \eta_\mu(t). \qquad (6)$$

Here we have considered, for convenience, a spatially uncorrelated random field. The autocorrelation and response functions become

$$C(t,t') = \int_{-2}^{2} d\mu \rho(\mu) \langle s_\mu(t) s_\mu(t') \rangle,$$

$$R(t,t') = \frac{1}{2T} \int_{-2}^{2} d\mu \rho(\mu) \langle s_\mu(t) \eta_\mu(t') \rangle, \qquad (7)$$

where $\rho(\mu) \equiv \sqrt{4 - \mu^2}/2\pi$ for $\mu \in [-2,2]$, and zero otherwise, is the density of eigenvalues of the random matrix J_{ij}. The spherical condition reads $C(t,t) = 1$, and, after projection, the amplitude of the field h_μ is random with zero mean and variance $\overline{h_\mu h_{\mu'}} = h^2 \delta_{\mu\mu'}$.

C. Fluctuation-dissipation relation and effective temperatures

We shall be interested in the fluctuation-dissipation theorem (FDT) and its possible modifications. For driven systems, we do not expect this relation to be satisfied. In equilibrium, *any* correlation function $C(t,t') = \langle O(t) O(t') \rangle$ [we assume, without loss of generality, that $\langle O(t) \rangle = 0$], and its associated linear response $R(t,t') = \delta \langle O(t) \rangle / \delta f(t')|_{f=0}$, where the perturbation f modifies the Hamiltonian of the system according to $H \to H - fO$, satisfy the FDT:

$$R(t,t') = \frac{1}{T} \frac{\partial C(t,t')}{\partial t'}, \quad t \ge t'. \qquad (8)$$

For nonequilibrium systems, a possible extension is [50,52]

$$R(t,t') = \frac{1}{T_{\text{EFF}}(t,t')} \frac{\partial C(t,t')}{\partial t'}, \quad t \geq t'. \quad (9)$$

Naively, this equation is simply a definition of the two-time function $T_{\text{EFF}}(t,t')$. This extension becomes nontrivial when one realizes that, in the long waiting-time limit of many solvable models, this function only depends on times via the correlation function itself:

$$T_{\text{EFF}}(t,t') = \mathcal{T}_{\text{EFF}}[C(t,t')]. \quad (10)$$

By extension, it has been proposed that this exact result for solvable, mean-field-like models, will also apply to more realistic models with, e.g., finite range interactions. Graphically, a convenient way of checking this ansatz is to represent the integrated response function $\chi(t,t') \equiv \int_{t'}^{t} dt'' R(t,t'')$ as a function of $C(t,t')$ at fixed t', and parametrized by the time difference $t-t'$ [53]. Equation (10) implies that a master curve (i.e., independent of t') $\chi(C)$ is asymptotically reached.

In the aging case, three families of models have been found [11]: (1) glassy models, for which the $\chi(C)$ curve is a broken straight line with a first piece, from $C=1$ to $C=q_{EA} \equiv \lim_{t\to\infty} \lim_{t'\to\infty} C(t,t')$, of slope $-1/T$ and a second piece, from $C=q_{EA}$ to $C=0$, of slope $-1/T_{\text{EFF}}$, T_{EFF} being finite; (2) ''domain growth models,'' for which the $\chi(C)$ curve is still a broken straight line with the second piece having $T_{\text{EFF}}=\infty$; and (3) spin-glass models, for which the $\chi(C)$ curve has a straight line piece from $C=1$ to $C=q_{EA}$ and a curved piece from $C=q_{EA}$ to $C=0$.

The modification of these plots in a system driven by shearlike forces was studied at the mean-field level in Refs. [18,21]. Numerically, the same behavior was found in a sheared supercooled liquid [39]. Finally, Langer and Liu studied a sheared foam, and studied the FDT by comparing the fluctuations of the stress on the boundary and the corresponding compression modulus [54].

At the theoretical level, it was shown in Ref. [52] that the factor T_{EFF} is indeed a *bonafide* temperature: it is commonly called the ''effective temperature.'' A very appealing connection of this factor with the ideas of Edwards [38], in the context of granular matter, and Stillinger and Weber [55] in the context of glass forming liquids, are currently being explored [56–58]. We shall come back to this point below.

Finally we wish to recall a rigorous bound that controls the maximum deviation from the FDT that can be observed in an out of equilibrium system with Langevin dynamics [59]. When a time-dependent force of period τ is applied on the system, the bound takes the form

$$\left| \int_{t_w}^{t_w+\tau} ds \left(\frac{\partial C(t,s)}{\partial s} - TR(t,s) \right) \right|$$
$$\leq \sqrt{\left(\mathcal{N} \int_{t_w}^{t_w+\tau} ds D^2(t,s) \right) \left(\frac{W}{N} \right)}, \quad (11)$$

where W is the total work done by the external force $\boldsymbol{h}$ on the system, per period, $W \equiv \int_{t}^{t+\tau} ds \langle \boldsymbol{v}(s) \cdot \boldsymbol{h}(s) \rangle$, $\mathcal{N}$ is a system

dependent numerical factor, and $D(t,s)$ is a two-time correlation that in most cases of interest is again bounded by a numerical constant. In particular, for the model we treat in this paper, both $\mathcal{N}$ and $D^2(t,s)$ are equal to 1. Hence, for this model, we have

$$\left| \int_{t_w}^{t_w+\tau} ds \left(\frac{\partial C(t,s)}{\partial s} - TR(t,s) \right) \right| \leq \sqrt{\tau \left(\frac{W}{N} \right)}. \quad (12)$$

D. Zero-drive dynamics: jammed states and Reynolds dilatancy

In the absence of a driving force, the model has a dynamical transition at a (p-dependent) critical temperature T_c. For instance, $T_c=1$ for $p=2$ and $T_c \simeq 0.6123$ for $p=3$. Above T_c, the equilibration time is finite, and the system reaches equilibrium. In this case, both time-translation invariance (TTI) and the FDT are satisfied, and Eqs. (4) reduce to a mode-coupling equation for the so-called F_{p-1} model [11,43,60]. The relaxation time diverges at T_c, and, below T_c, the system does not equilibrate with its environment. A quench from the high temperature phase toward the low temperature phase is followed by the aging dynamics described in Sec. I: the relaxation time increases with t_w, which means that the TTI is lost. The FDT is modified in the way described in Sec. II C. One-time quantities have a slow relaxation, typically power laws, and, for instance, the energy density converges to a value $e(t\to\infty)=e_{th}(T)$ which is higher than the equilibrium value $e_{eq}(T)$.

From the static point of view [44,61], T_c is the temperature below which the energy landscape becomes fractured into many metastable states. ''Many'' means that their number $\mathcal{N}(T,e)$ is such that the thermodynamic limit

$$\lim_{N\to\infty} \frac{\ln \mathcal{N}(T,e)}{N} \quad (13)$$

exists and is finite. The so-called complexity (or ''configurational entropy'') $\Sigma(T,e) \equiv \ln \mathcal{N}(T,e)$ is hence *extensive* in a range $e \in [e_{eq}(T), e_{th}(T)]$. The effective temperature T_{EFF} defined in the Sec. II C from FDT violations can be computed directly from the dynamical equations. A remarkable result is that it is also given by [62]

$$\frac{1}{T_{\text{EFF}}} = \left. \frac{\partial \Sigma(T,e)}{\partial e} \right|_{e=e_{th}} \quad (14)$$

at $T=0$. [At finite temperature the free energy density replaces the energy density in Eqs. (13) and (14).] This relation is very similar to the thermodynamic definition of temperature, and to the definition of Edwards' compactivity in granular systems. We shall come back to these similarities in Sec. VI.

The complexity is a useful quantity for understanding, for example, the difference between the dynamics of the $p=2$ and $p \geq 3$ models. For $p=2$, one has $e_{eq}=e_{th}$, and the complexity is irrelevant, $\Sigma=0$. It follows that $T_{\text{EFF}}=\infty$. This

case falls in the "domain growth family" defined in Sec. II C. Instead, if $p \geq 3$, $e_{eq} < e_{th}$, $\Sigma > 0$ in the region $[e_{eq}, e_{th}]$, and T_{EFF} is finite.

If, instead of a quench from a high temperature at $t=0$, the dynamics starts from one of the metastable states with energy density $e_{eq} < e < e_{th}$, the system may escape this state, but on a time scale which diverges with N. The ergodicity is broken, and the dynamics is blocked. We could call these metastable states the "jammed states" of the system. (They are known as Thouless-Anderson-Palmer states in the spin glass literature [61].)

When a driving force is applied to the system, the dynamics also depends on the initial state. The driven dynamics following a quench under shearlike forces was investigated in Refs. [18,21]. When starting from a low-lying state, and *for a small enough driving force*, the system remains trapped (jammed). Only by applying a large force will the system escape the deep state and have a dynamics like the one following a quench [18]. Hence the system becomes able to move only by raising its energy density: this is, in the glassy context, the Reynolds dilatancy effect [1,10].

The effect of these trapping states on the dynamics following a quench are beyond the mean-field approximation [Eqs. (4)]. We propose to investigate this interesting aspect by simulating, in Sec. IV C, the Ising version of the model, keeping *finite* the number N of interacting spins, so that jammed states will be dynamically accessible by the system.

III. DRIVEN SPHERICAL SHERRINGTON-KIRKPATRICK MODEL

In this section we study analytically the driven dynamics of the $p=2$ case.

A. Existence of a dynamic transition

Let us first study the $p=2$ case at $T=0$. The Langevin equation (6) can be integrated out; this yields

$$s_\mu(t) = \frac{e^{\mu t}}{\Omega(t)} \left[1 + h_\mu \int_0^t dt' \cos(\omega t') e^{-\mu t'} \Omega(t') \right],$$
(15)

where the function

$$\Omega(t) \equiv \exp\left[\int_0^t dt' z(t') \right]$$
(16)

has been defined. The spherical constraint determines $\Omega(t)$ through the equation

$$\Omega(t)^2 = f(t) + h^2 \int_0^t dt' \int_0^t dt'' f\left(t - \frac{t' + t''}{2} \right)$$
$$\times \Omega(t') \Omega(t'') \cos(\omega t') \cos(\omega t''),$$
(17)

with $f(t)$ given by

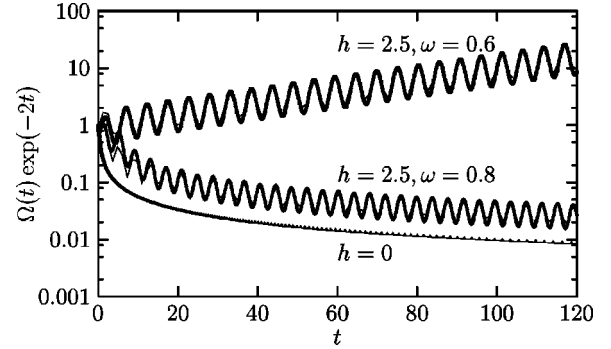$$f(t) \equiv \int_{-2}^{2} d\mu \rho(\mu) e^{2\mu t}.$$
(18)

FIG. 1. The function $\Omega(t) \exp(-2t)$ in the three cases $h=0$, $h=2.5$ and $\omega=0.8$ (glassy phase), and $h=2.5$ and $\omega=0.6$ (liquid phase), from bottom to top. The points are the direct integration of Eq. (17), while the full lines are fits to Eqs. (20). Except at very short times, the approximate forms in Eqs. (20) yield the correct behavior.

The autocorrelation and response functions, together with the energy density, read

$$C(t, t_w) = \frac{1}{\Omega(t) \Omega(t_w)} \left[f\left(\frac{t + t_w}{2} \right) \right.$$
$$+ h^2 \int_0^t dt' \int_0^{t_w} dt'' \cos(\omega t') \cos(\omega t'') \Omega(t')$$
$$\left. \times \Omega(t'') f\left(\frac{t + t_w - t' - t''}{2} \right) \right],$$

$$R(t, t_w) = \frac{\Omega(t_w)}{\Omega(t)} f\left(\frac{t - t_w}{2} \right),$$
(19)

$$e(t) = -\frac{z(t)}{2} = -\frac{1}{2} \frac{d \ln[\Omega(t)]}{dt}.$$

Equation (17) determines $\Omega(t)$ and, consequently, all dynamic quantities. Unfortunately, it cannot be completely solved analytically except in some asymptotic limits.

Two special cases have been studied previously, namely, the zero field behavior of the model, and the case of a dc field. In the former, as discussed in Sec. II, there is no finite equilibration time below $T_c = 1$ and the system ages forever [46,47]. In the presence of a dc magnetic field of amplitude h [48], Eq. (17) yields $\Omega(t) \sim \exp[\lambda^0(h)t]$, where $\lambda^0(h) \equiv (2 + h^2)/\sqrt{1 + h^2}$. The main effect of the field is to introduce a new time scale $t_r^0(h) \equiv [\lambda^0(h) - 2]^{-1}$ in the problem. For times $t_w \ll t_r^0(h)$ after the quench, aging is observed as in the zero-field case, whereas at later times $t_w \gg t_r^0(h)$ the system has reached its equilibrium state in a field: aging is interrupted. The energy density $e(t)$ converges to $e_\infty(\omega=0, h) = -(2 + h^2)/(2\sqrt{1 + h^2})$.

At finite ω, the numerical solution of Eq. (17) displayed in Fig. 1 suggests the following asymptotic behavior:

$$h < h^\star(\omega), \quad \Omega(t) \sim c \frac{e^{2t}}{t^{3/4}} [b \cos(2\omega t + \phi) + 1],$$

$$(20)$$

$$h > h^\star(\omega), \quad \Omega(t) \sim c' \exp[\lambda(\omega,h)t + a \cos(2\omega t + \phi)],$$

where c, c', a, $b < 1$, and ϕ are numerical constants, and with $\lambda(\omega,h) > 2$. This means that if the amplitude of the driving force is sufficiently small, the ac field does not introduce a new time scale, and a full aging behavior is observed. For stronger amplitudes of the field, a time scale defined by

$$t_r(\omega,h) \equiv [\lambda(\omega,h) - 2]^{-1} \qquad (21)$$

is generated, and the relaxation time becomes finite: aging is stopped by the driving force. Hence there is a critical field $h^\star$ separating these two different regimes. It is clear from Fig. 1 that the agreement between Eqs. (20) and the numerical solution is very good, after a short transient. In the following we characterize these two phases, as well as the transition between them.

B. Transition line in the plane (ω, h)

We have seen that, at a fixed pulsation ω, there exists a well-defined transition line where the relaxation time in an ac field diverges, allowing one to distinguish between ''glassy'' and ''liquid'' states. We anticipate the discussion of Sec. III A to emphasize that this transition is a nonequilibrium phase transition, which is hence of a different nature that the transition taking place at T_c in the absence of the driving force.

The transition line $h^\star(\omega)$ may be understood and estimated from a simple physical argument. At $\omega = 0$, the dc field introduces a finite relaxation time $t_r^0(h)$. The most naive requirement for the system to retain a finite relaxation time in an ac field of period τ is given by $t_r^0(h) \lesssim \tau$. The transition line is then estimated by the relation

$$t_r^0(h^\star) \simeq \tau \Leftrightarrow \omega \propto \left[\frac{2 + h^{\star 2}}{\sqrt{1 + h^{\star 2}}} - 2 \right]. \qquad (22)$$

A more refined computation can also be performed. Using the fact that, when $h > h^\star$, $\Omega(t)$ is given asymptotically by Eq. (20) with $\lambda > 2$, allows us to neglect the term $f(t)$ on the right hand side of Eq. (17); thus

$$\Omega(t)^2 \simeq h^2 \int_{-2}^{2} d\mu \rho(\mu) e^{2\mu t} \left[\int_0^t dt' \cos(\omega t') \Omega(t') e^{-\mu t'} \right]^2. \qquad (23)$$

Inserting the form $\Omega(t) = \exp[\lambda t + B(t)]$, and formally integrating by parts, yields
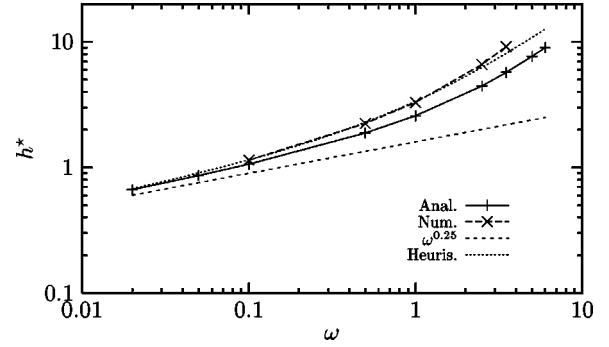

FIG. 2. The transition line $h^\star(\omega)$, estimated by analytical, numerical, and heuristic tools, together with the small frequency behavior $h^\star \propto \omega^{0.25}$.

$$e^{B(t)} = h^2 \int_{-2}^{2} d\mu \rho(\mu)$$

$$\times \left[\mathrm{Re} \left(e^{i\omega t} \sum_{k=0}^{\infty} \frac{(-1)^k}{(\lambda(\omega,h) - \mu + i\omega)^{k+1}} \cdot \frac{d^k e^{B(t)}}{dt^k} \right) \right]^2.$$

$$(24)$$

Since the function $B(t)$ is periodic with the angular velocity 2ω, this corresponds to a development in powers of ω. In the small frequency limit, the equation can be closed by keeping only the leading terms of the development, and this yields a relation between (λ, ω, h),

$$\frac{\pi}{h^2} = \int_{-1}^{1} dx \frac{\sqrt{1 - x^2}}{(\lambda - 2x)^2 + \omega^2}, \qquad (25)$$

from which we estimate the transition line where the time scale $t_r(\omega,h)$, given in Eq. (21), diverges. This is equivalent to the condition $\lambda(\omega, h^\star) = 2$. It is easily shown that, in the small frequency limit, the scaling $t_r^0(h^\star) \simeq \tau$ is recovered, in accordance with our heuristic argument [Eq. (22)]. In Fig. 2, the analytical estimate for the transition line $h^\star(\omega)$ is compared with its direct numerical estimation, and with our heuristic argument. Also plotted is the small frequency behavior of the critical field, $h^\star \propto \omega^{0.25}$.

Moreover, Equation (25) implies

$$\lim_{\omega \to 0} \lambda(\omega, h) = \lambda^0 \left(\frac{h}{\sqrt{2}} \right), \qquad (26)$$

which means that, in the limit $\omega \to 0$, the field acts as a constant field with an amplitude given by its root mean square value, which is physically reasonable. Importantly enough, this means that the effect of a dc field with ω strictly zero, and the limit of an ac field with vanishing frequency, are different. In the case $p = 2$ this feature has no effect on the value of the transition field $h^\star$, since it vanishes in both cases. However, when $p \geq 3$ we shall find a nontrivial consequence of this result (see Sec. IV).

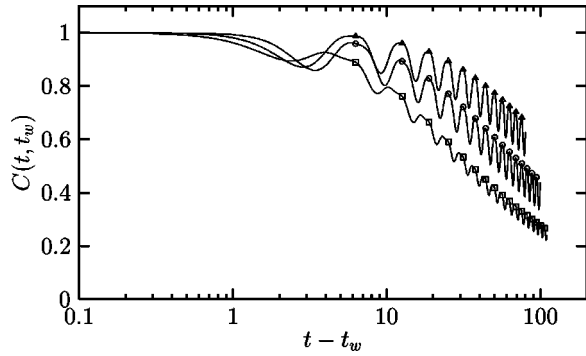FIG. 3. Correlation function of the $p=2$ model at $T=0$ for $h=0.5$ and $\omega=1$, and waiting times $t_w=5$, 10, and 20, from bottom to top. The points fall on the discrete times $t=n\tau$, with n an integer.

C. Below the transition $h<h^\star(\omega)$: aging in an ac field

Below the transition, Eq. (20) shows that the energy density slowly converges toward its asymptotic value $e_\infty(\omega,h<h^\star)=-1$ as a power law $e(t)-e_\infty\sim t^{-1}$ with a superimposed oscillation at a frequency ω/π. This asymptotic value is independent of h. A slow (here a power law) convergence of one time quantities is typical of aging systems [11]. The angular velocity 2ω is expected since Eq. (6) remains unchanged by the transformations $t\rightarrow t+\pi/\omega$, $s_\mu\rightarrow-s_\mu$, and $z\rightarrow z$. The constraint $z(t)$, and the energy density, are then π/ω periodic.

That the TTI is also lost is demonstrated by looking at two-time quantities, typically correlation functions. The behavior of $C(t,t_w)$ is represented in Fig. 3. This figure also shows the interesting feature that the dynamics can be decomposed into two well-separated time scales. At short time separation $t-t_w$, the time scale for the approach to the plateau at $C=q_{EA}$ (note that $q_{EA}=1$ at $T=0$) does not depend on t_w, whereas the decay from the plateau toward zero arises in a second time scale that clearly depends on t_w. During the waiting-time-dependent decay, the curves have oscillations. Quantitatively, the behavior of the correlation function is entirely dominated at long times by the term $C(t,t_w)\sim f[(t$
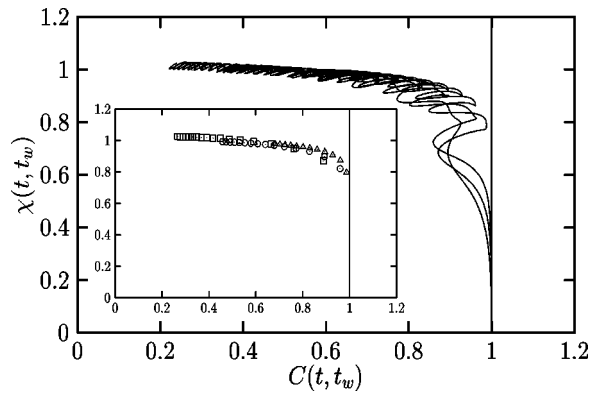

FIG. 4. Parametric plot of the integrated response correlation of the $p=2$ model at $T=0$ for $h=0.5$ and $\omega=1$, and waiting times $t_w=5$, 10, and 20. For the FDT to be satisfied, the points have to lie on the vertical line. The inset represents the same data, but for times $t=n\tau$; the symbols are the same as in Fig. 3.
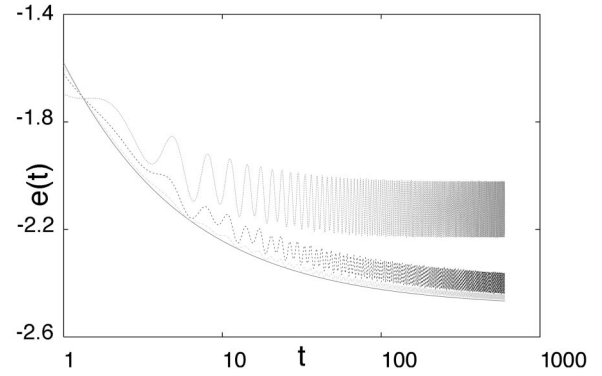

FIG. 5. Time dependence of the energy density under an ac field with amplitude $h=0$, 0.3, 0.6, and 1 (from bottom to top), and angular velocity $\omega=1$. The curve for $h=1$ approaches rapidly an asymptote, whereas $e(t)$ still evolves at large times for the other cases.

$+t_w)/2]/[\Omega(t)\Omega(t_w)]$. This implies that, apart from the oscillation, the correlation scales as t/t_w for $t\gg t_w$; we have checked this point numerically.

In tapping experiments, data are obtained for times of the form $t=n\tau$, where n is an integer. We have represented these data by points in Fig. 3, and the experimental measurements would be very similar to the usual aging case.

The response function is analyzed in Fig. 4, where the parametric plot of the integrated response against the correlation is built. As expected, there are strong violations of the FDT. However, these violations are similar to those encountered in the relaxational case, in the sense that there are two distinct behaviors, depending on the time scale considered. For a time separation $t-t_w\ll t_w$, the FDT is not satisfied, and no effective temperature can be defined. For the second time scale $t\gtrsim t_w$ and longer, on the contrary, all points fall nicely on a straight line, with a superimposed oscillation. Bound (12) shows, however, that the deviation from the FDT can only be significant at large times, when both $\partial C(t,t_w)/\partial t_w$ and $R(t,t_w)$, integrated over a period, are small. This is confirmed by Fig. 4.

The inset of Fig. 4 shows $\chi(C)$ for the discrete times $t=n\tau$. If one uses this stroboscopic measurement, it remains clear that the FDT modifications are well accounted for by ansatz (10). Analytically, neglecting, as above, the second term in the correlation function, the effective temperature defined through Eq. (9) scales as $T_{EFF}\sim t_w^{1/2}\rightarrow\infty$. An infinite effective temperature is also present in the relaxational dynamics of this model, and is typical of domain growth models.

With these simple considerations we have argued that the effect of a small ac field does not change the aging behavior of this model at $T=0$. This is to be confronted to the effect of non-Hamiltonian perturbations that change the aging scaling, as seen, for instance, in the correlation function that becomes $C(t,t_w)\sim f[\exp(\sqrt{t_w}-\sqrt{t})]$ [18]. At nonzero temperature, shearlike forces introduce a finite relaxation time, after which the dynamics is stationary. We have not solved the $p=2$ model analytically at finite temperature in an ac field, but the numerical solution of the full equations sug-
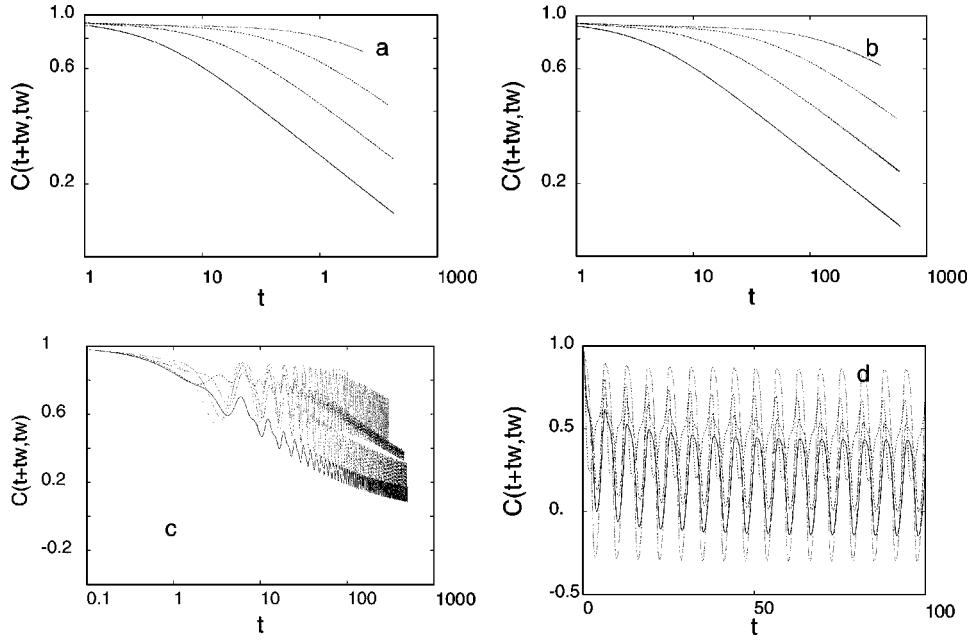
FIG. 6. Each panel shows the autocorrelation $C(t+t_w,t_w)$ as a function of t, for four values of the waiting time $t_w=3$, 12, 49, and 198, at $T=0.2$. The angular velocity of the applied field is $\omega=1$. In panels (a)–(c) the scale is logarithmic, the amplitudes of the applied fields are $h=0$, 0.1, and 1, and the system is in its glassy phase. In panel (d) the scale is linear, $h=2$, and the slow dynamics is suppressed.

gests that there is a finite region of the phase diagram (T,h,ω) in which aging effects survive. This explicitly shows that the effects of shear and tapping are rather different.

D. Above the transition: Driven steady state

Above the transition, the situation is simpler. After a time scale $t_r(\omega,h)=[\lambda(\omega,h)-2]^{-1}$, the slow dynamics is lost. Relation (25) implicitly determines λ, which is an increasing function of the amplitude h of the driving force. In the stationary state, the energy density oscillates with an angular velocity 2ω around its asymptotic value $e_\infty(\omega,h>h^\star)=-\lambda(\omega,h)/2$. The behavior of the correlation is dominated by the second term in Eq. (19). This shows that it decays toward zero on a time scale of order $t_r(\omega,h)$: there is no more aging.

IV. BEHAVIOR FOR $p \geqslant 3$

Going beyond the solution of the unperturbed case [50] to solve the set of coupled integro-differential equations (4) analytically is a very hard task. In order to illustrate the main properties of the solution, we solved Eqs. (4) numerically, by constructing a two-time solution step by step in time. We first demonstrate that in the case $p \geqslant 3$, there also exists a transition line below which glassy properties of the undriven model persist, and then study the FDT violations in both phases.

A. Evidence of a dynamical transition

Let us recall first the effect of a dc magnetic field of amplitude h on the system [63]. In contrast to the spherical
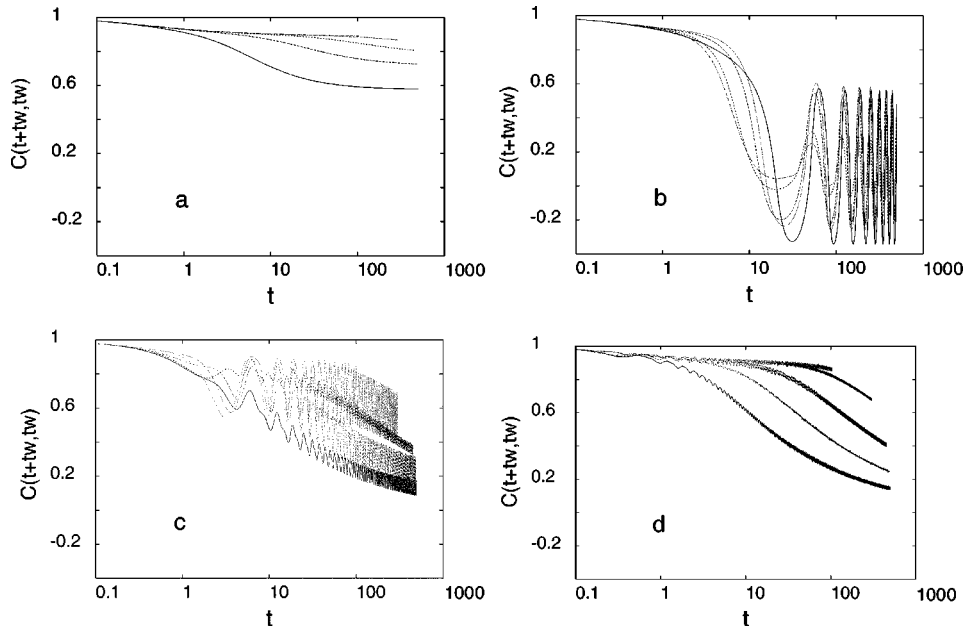

FIG. 7. Each panel shows the autocorrelation $C(t+t_w,t_w)$ as a function of t, for four values of the waiting time $t_w=3$, 12, 49, and 198 at $T=0.2$. The strength of the applied field is $h=1$ and the frequencies are $\omega=0$, 0.1, 1, and 10 from panels (a) to (d). The transition in an ac field of amplitude $h=1$, from the liquid to the glassy phase, occurs at a frequency $0.1<\omega_c<1$.
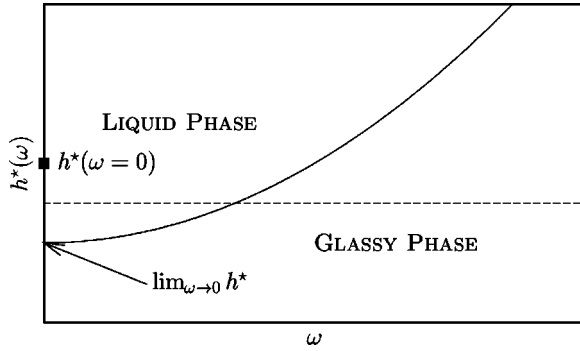
FIG. 8. The full line is a schematic representation of the transition line $h^\star(\omega)$ for $p \geq 3$. The angular velocity in the four panels in Fig. 7 move from left to right along the horizontal dashed line (see the text for more details).

Sherrington-Kirkpatrick model, the spin glass phase may exist in a dc magnetic field. There are both dynamic and static transitions between the spin glass and the paramagnetic phases. At $T = 0.2$, the dynamic transition takes place at $h^\star(\omega = 0) \simeq 1.1$ [63].

As in the case $p = 2$, we begin our study by focusing on the behavior of the energy density $e(t)$. This is displayed in Fig. 5 at temperature $T = 0.6$ and angular velocity $\omega = 1$, for different field amplitudes. The long time behavior of $e(t)$ indicates that the transition occurs for a field $0.6 < h^\star < 1.0$ at this frequency. The asymptotic value of the energy density increases slightly below the transition, and reaches a much larger value, when $h > h^\star$.

In the following we concentrate on the temperature $T = 0.2 \simeq 0.32 T_c$, i.e., well below the zero-field transition. We focus first on the dependence of the two-time autocorrelation functions on the amplitude of the applied field. In Fig 6(a), the field is $h = 0$, and we observe the usual aging [50]. It is then clear that aging is still present if the field is not too strong, $h = 0.1$ and 1 in Figs. 6(b) and 6(c), whereas at a stronger field, $h = 2$ in Fig. 6(d), the correlation tends very rapidly to zero, with a superimposed oscillation. These observations reinforce the evidence in favor of a dynamic transition which, at $T = 0.2$, occurs at a field strength $1 < h^\star < 2$ for $\omega = 1$.

We turn now to the question of identifying the critical line in the ω direction. Figure 7 shows the autocorrelation function at fixed amplitude of the applied field and several values of the angular velocity. In Fig. 7(a), the frequency is zero, and aging is observed with a two-step decay of the correla-

tion. Note that the second decay is toward a value $q_0 > 0$, as opposed to the zero-field case [63]. The frequency is increased in Figs. 7(b)–7(d). At intermediate frequency [Fig. 7(b)], aging is suppressed. When ω is further increased [Figs. 7(c) and 7(d)] it is clear that the glassy phase is reentrant.

It is of course very difficult to determine the transition line $h^\star(\omega)$ with accuracy by the numerical solution of the dynamical equations. We are hence not able to draw a figure similar to Fig. 2 for $p \geq 3$. In Fig. 8 we show a schematic representation of this critical line with the feature, already encountered for $p = 2$, that the limit $\omega \to 0$ is peculiar. From the numerical solution at $\omega > 0$, it seems that

$$\lim_{\omega \to 0} h^\star(T, \omega) < h^\star(T, \omega = 0). \tag{27}$$

This is represented in Fig. 8, and explains the reentrance of the glassy phase described in Fig. 7, when the frequency increases. Note, however, that we cannot numerically discard the possibility of a nonmonotonic, but smooth, behavior of the critical line at $\omega < 0.1$.

B. Fluctuation-dissipation theorem

We now turn to a study of the FDT. In Fig. 9 we show the evolution of the χ vs C plots with t_w. In Fig. 9(a), the system is not in a glassy phase. Strong violations of the FDT are observed, but no effective temperature can be defined. The system is athermal.

In Fig. 9(b), conversely, the system is in its glassy phase. One then recovers a $\chi(C)$ curve that is very similar to the one in zero field. The first part is almost a straight line with slope $-1/T$, while the second decay follows a temperature $-1/T_{EFF}$. As mentioned in Sec. III, the fact that, for small time scales, the FDT is nearly satisfied results directly from bound (12).

The nontrivial outcome of this study is the fact that a well-defined T_{EFF}, which exists in the nondriven system, may still be defined below the dynamical transition, in the presence of the drive. A stroboscopic construction, like the one in Sec. III C, will yield a perfect straight line that defines T_{EFF} unambiguously.

The actual value of the effective temperature may depend on various parameters. We have searched for dependences on the frequency and amplitude of the ac field. Within the range of parameters we could numerically explore, we have not observed large dependences. Figure 10 displays the χ vs
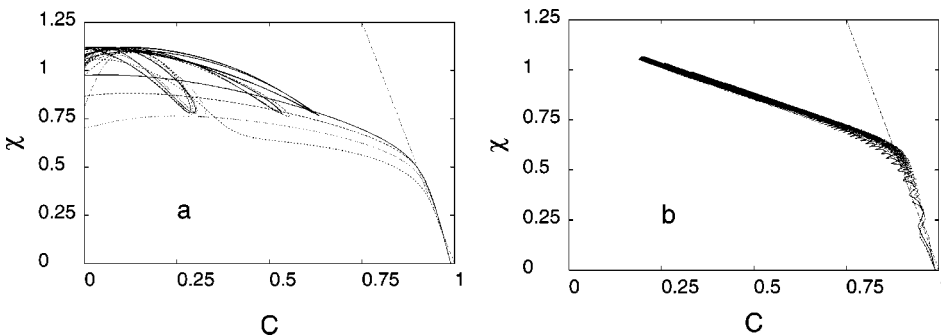

FIG. 9. The $\chi(C)$ curves at $T = 0.2$ with an applied ac field of strength $h = 1$ and frequencies $\omega = 0.1$ (liquid phase) and $\omega = 10$ (glassy phase), for different waiting times $t_w = 6$, 12, 24, and 49.
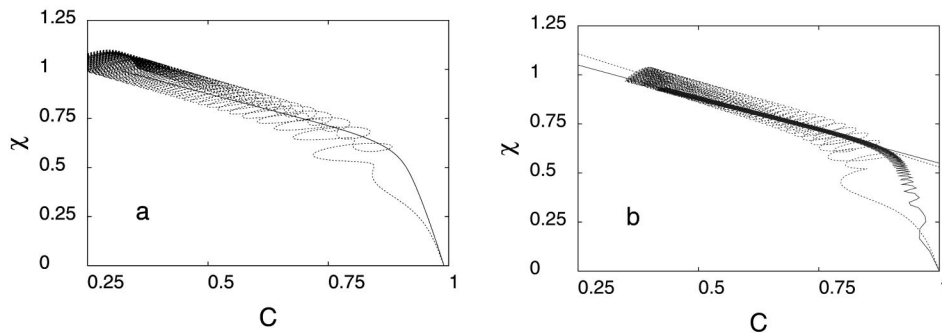
FIG. 10. The $\chi(C)$ curves at $T=0.2$. In panel (a), the two curves correspond to $h=0$, and $h=1$, and $\omega=1$. In both cases the system is in its glassy phase. In panel (b) the two curves correspond to $\omega=1$ and 10, both with an amplitude $h=1$. The lines are guides to the eye, and they have the slope of the second part of the decay. $t_w=24$ for all curves displayed.

C curves for two choices of field amplitudes, and for two choices of angular velocity at fixed field amplitude, the dependence is indeed weak.

C. Beyond the mean field: effect of trapping states

In this section we present results from a numerical simulation of the Ising version of the p-spin model in an ac field, in the particular case $p=3$. We focus on the time dependence of the energy density $e(t)=N^{-1}\Sigma_{i<j<k}J_{ijk}s_is_js_k$ and the magnetization density $m(t)=N^{-1}\Sigma_i s_i(t)$. The sizes $N=50$ and 150 have been used, together with a constant temperature $T=0.01$, in all simulations. The amplitude and the frequency of the magnetic field have been varied.

The interest of such an investigation is that the finite N behavior of the model is accessible. The system is hence able to escape and visit the trapping states described in Sec. II in a finite time [18]. For this reason, the results presented in this section cannot be obtained in a mean-field approach.

In the absence of magnetic field, the energy density rapidly approaches its asymptotic value. At such a low temperature, the system reaches a metastable stable, characterized by a nearly zero magnetization density, and cannot escape within the numerical time window. Figure 11 (left) illustrates this ''jammed'' behavior. The value of the energy density depends on the initial conditions, which means that the system may be blocked in different trapping states when it starts from different initial conditions.

The influence of an ac magnetic field on this jammed behavior is evident in Fig. 11 (right). Both the energy and the magnetization density are oscillating functions, and their behavior is intermittent. For some time windows, both quantities have an evolution which varies considerably from period to period. For other time windows, conversely, the different cycles are very similar. This can be interpreted as being due to the presence of the trapping (jammed) states: the system usually evolves inside one of the trapping states, without escaping, and all the periods are equivalent. However, from time to time, the driving force is able to make the system escape the state, and the evolution is very erratic until another trapping state is found.

This is confirmed in Fig. 12, where the energy density is represented as a function of t for times of the form $t=n\tau$. The long horizontal plateaus are the moments where the system is jammed, whereas, between the plateaus, the energy density changes values very rapidly. As in Ref. [18], in Fig. 12 we show that the time evolution of $e(t)$ is ''self-similar,'' in the sense that zooming on a time window makes smaller plateaus become visible while the overall evolution looks the same.

This intermittent behavior is clearly reminiscent of the behavior encountered in some granular experiments, where the powder is very slowly perturbed, like the ones performed by the Jussieu group [64]. In particular, it would be very interesting to perform a more careful analysis of the statisti-
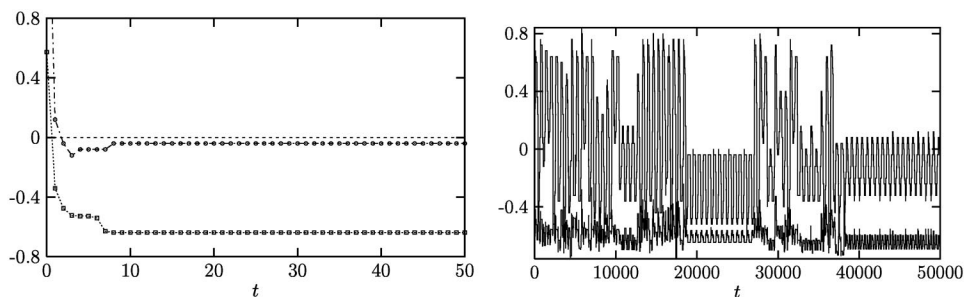

FIG. 11. Evolution of the energy (bottom curve) and magnetization (top curve) densities without (left) and with (right) magnetic field. The parameters of the field are $h=2$ and $\omega=0.01$. Note that the time range in the left figure is much shorter, since both $e(t)$ and $m(t)$ are constant for times $t>50$.
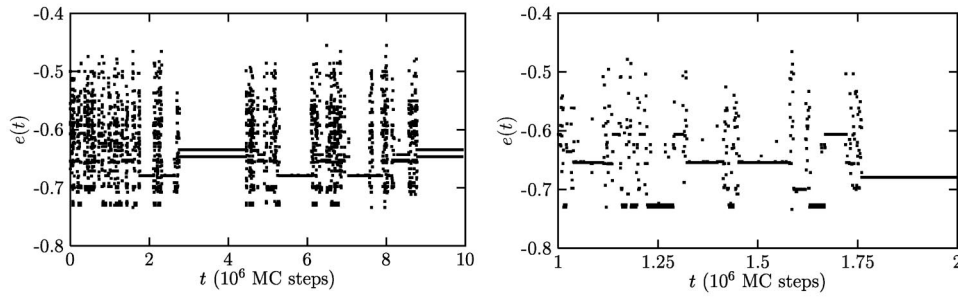
FIG. 12. Same parameters as in Fig. 11. Evolution of the energy density with a magnetic field. Only one point per period is represented.

cal properties of $e(t)$ such as, e.g., measuring the statistics of trapping times [64]. We also note that this phenomenology is very similar to the one of the so-called ''trap model'' [65], that was extended by Head to describe the phenomenology of granular materials [36].

Finally, it is interesting to stress that even within one cycle of the field, the evolution is not regular at all. This can be seen nicely in Fig. 13, where the field $h(t)$ is represented as a function of the magnetization $m(t)$. This is the usual view of a hysteresis loop in ferromagnetic systems. It is clear that the shape of the loops is far from elliptic, and that the system evolves in steps, rather than continuously: this is analogous to the Barkhausen noise [66]. The overall shape of a cycle depends drastically on whether the system is trapped or not. It is beyond the scope of this paper to study these loops in detail, but we emphasize that this (mean-field) model could be an interesting starting point to study the Barkhausen noise, in the spirit of Ref. [66].

V. SUMMARY AND LINK WITH GRANULAR MATTER

Phase diagram. Our findings concerning the behavior of glassy systems under a time-dependent driving force are summarized in Figs. 8 and 14. For any fixed frequency of the

applied field, and a temperature $T<T_c$, where T_c is the zero-drive glass transition temperature, there are two regimes: (I) At small drive, the system exhibits slow (''glassy'') dynamics. (II) At large drive, there is no slow dynamics. There then exists a well-defined critical drive separating these two regimes. On the other hand, if we work at a fixed drive and modify the angular velocity, the system undergoes a transition from a liquidlike phase at low (though nonvanishing) frequency to a glasslike phase at high frequency. This result is displayed in Fig. 8.

The phase diagram in Fig. 14 is the analog to the (T,Γ) plane of the three-dimensional phase diagram proposed by Liu and Nagel [7]. We have then investigated its properties in detail, which to our knowledge has not been done so far in the case of a time-dependent driving force. Contrary to previous phenomenological modelings of the dynamics of granular matter, assuming that the drive Γ is related (in a possibly nonlinear way) to the temperature T of a glassy model borrowed from statistical mechanics, here we propose to study precisely the interplay between T and Γ as an intermediate step from glassy to granular materials. The conclusions we draw are then directly pertinent to gently driven granular materials or slow granular rheology.
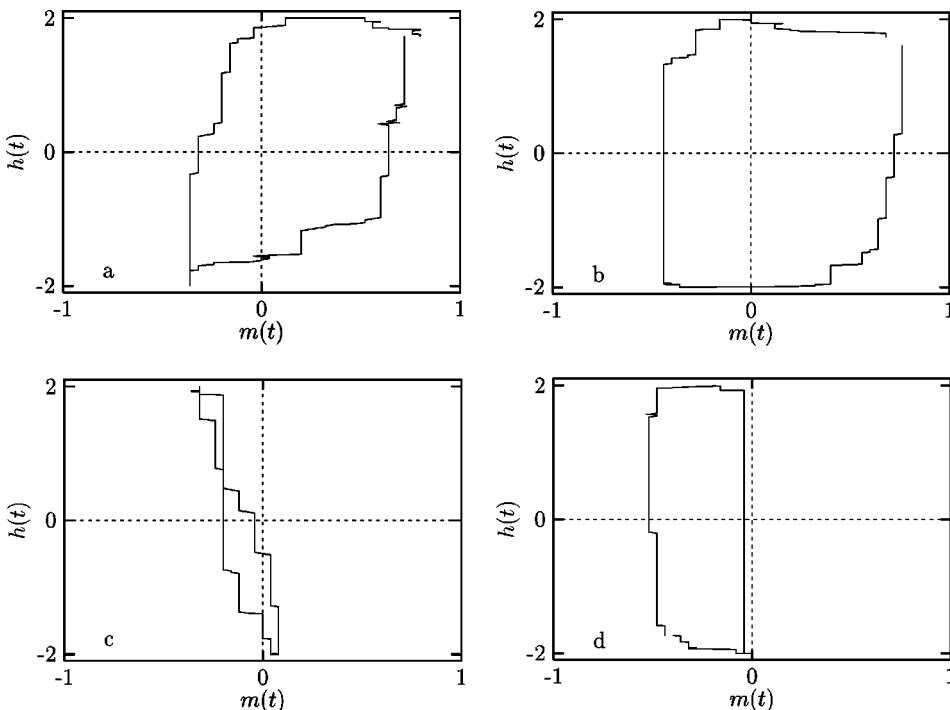

FIG. 13. Hysteresis loops. Panels (a) and (b) correspond to the period of rapid motion, while panels (c) and (d) correspond to interval when the system is trapped. $N=50$, $T=0.01$, $h=2$, and $\omega=0.1$.
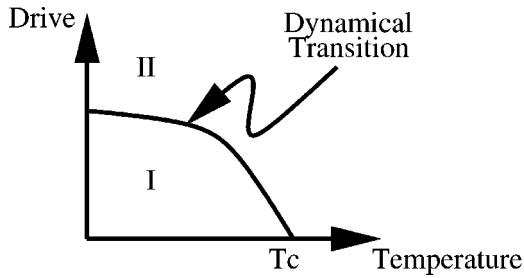
FIG. 14. Temperature-drive phase diagram of a glassy system. The vertical axis represents the typical amplitude of the driving force: its precise definition depends on the specific experiment considered; T_c is the zero-drive glass transition temperature.

We emphasize once again that the model we have studied is *not* intended to describe granular matter in full microscopic detail, but rather to act as a source of inspiration for the interpretation of numerical and experimental results. It may also motivate new experimental measurements. However, let us briefly summarize its dynamic behavior in the context of existing data for granular matter.

One-time quantities. In phase (I), one-time quantities (we have focused on the energy density) typically decay toward their asymptotic values as power laws. It is experimentally established that the density $\rho(t)$ in a gently driven granular system exhibits a very slow relaxation [1]. The parallel can be drawn with the energy density $e(t)$ [or more precisely with $-1/e(t)$] in glassy models. The seminal experiments at Chicago exhibited a logarithmic relaxation of the density [2], as found in all subsequent works [4,26–32,34–36]. (Note that Ref. [2] explicitly excluded a power law behavior.) However, the recent experiment of Nicolas *et al.* [3] showed that the logarithmic law is *not* a universal behavior, and that the time dependence may depend on the way the system is perturbed. From a theoretical point of view, one could prefer a power law decay for any one-time quantity, since it does not involve an intrinsic time scale, whereas the logarithmic law $1/\ln(t/t_0)$ explicitly introduces a time scale t_0. In this context, it is interesting to note that Barrat and Loreto [28], in their study of the Tetris model, showed that the fitting parameter t_0 actually depends on the considered time window; qualitatively $t_0 \propto t_w$. Head [36] already emphasized the role of the time window on the fitting parameters, in particular on the asymptotic value of the density.

In the context of glassy systems, it is a well-known feature that the interpretation of data over a finite time window is always delicate. A typical example is provided by the case of dipolar glasses, where the dielectric constant for samples prepared with different cooling rates seems to approach different asymptotic values [15].

Two-time quantities. In phase (II), the model we have studied also exhibits aging. For $p=2$, we find a t/t_w scaling (in stroboscopic time) of the autocorrelation function, while for $p \geq 3$ a much more careful numerical analysis is needed to determine this law. Other glassy models perturbed with ac forces may lead to other aging scalings. Generally speaking, theoretical arguments [11] indicate that one can expect the following behavior for any two-time function $F(t,t_w)$,

$$F(t,t_w) \sim \mathcal{F}\left(\frac{h(t)}{h(t_w)} \right), \qquad (28)$$

in a given time scale. $\mathcal{F}$ and h are two model- system-dependent scaling functions. More complicated scalings, such as a sum of different terms like Eq. (28), implying several different time scales in the problem, are also possible.

Two-time quantities such as the density-density correlation function were numerically studied, clearly demonstrating that the TTI is lost [27,31,28]: the Tetris model exhibits a $\ln(t)/\ln(t_w)$ behavior [27,28], whereas the parking lot model shows a t/t_w aging behavior [31].

An experimental determination of the scaling of two-time quantities will be useful to discriminate among the different models proposed to describe granular matter. This was already proposed in Refs. [27,28,31], and amounts to an experimental determination of the function $h(t)$ involved in Eq. (28). Such experimental determinations in glassy systems are by now numerous. They have emphasized, on the one hand, the universality of the aging phenomena in many microscopically different systems [12–16]; however, on the other hand, they have also revealed subtle differences between them [11,13].

Fluctuation-dissipation theorem violations. Our study has shown that modifications of the FDT, rather similar to those observed for *aging* glassy systems, also arise in glassy models driven by time-dependent forces. The parallel with granular materials suggests that this may also happen in driven powders.

The parametric plot we have built clearly shows that driven glassy systems have two distinct time scales, which we interpret as in Refs. [8,9]. A fast one, which is essentially independent of the waiting time, represents the individual motion of grains: no effective temperature, in the sense of Eq. (9), can be defined here. Since the model we have used is itself thermal (it uses a Langevin equation with a thermal noise), the fast motion has a reminiscence of the temperature of the bath (that may be zero). In a more realistic model of granular matter, it is likely that the fast motions will be completely athermal. Conversely, the long time scale, growing with the waiting time and giving rise to the t/t_w relaxation, represents large structural rearrangements in the powder. Our results indicate that these slow degrees of freedom are thermalized at a well-defined effective temperature. We are confident that this result also holds in realistic models of granular matter.

Again, numerical and experimental work could be used to check these predictions in granular materials. We have shown that the two models studied here have different FDT violations: the $p=2$ case has an infinite effective temperature, whereas the $p \geq 3$ models have a single finite effective temperature. Other glassy models (for instance mean-field spin glasses) have been shown to have a hierarchy of effective temperatures when they are undriven, and shall probably keep this behavior under driving forces [67]. We conjecture that granular materials fall in the $p \geq 3$ category, by analogy with structural glasses. This prediction has to be tested experimentally and numerically. It is not unlikely that different

microscopic models lead to different FDT violations; such a numerical determination could once again discriminate between them.

To study FDT violations during the compaction experiment, one has to compute, separately, the correlation function between two observables and its conjugated response function. In experiments for instance, the Nyquist relation is checked through dielectric measurements [14,68]. In granular materials, a natural choice is to check the Einstein relation between self-diffusion and the mobility of the grains. The results obtained in Refs. [69,70] are then very encouraging, although the driving field is not time dependent in these studies. Nicodemi instead studied the fluctuation-dissipation relation between height-height displacement, and its conjugated integrated response to small shaking amplitude perturbations in the Tetris model [71]. In the low density regime (fluidelike), after a short transient, these two quantities are related by the usual FDT. In the high density regime, the relation between these quantities shows much stronger deviations from the FDT than the model we studied here. This difference may be due to the kind of perturbation used by Nicodemi. For a thermal system, the procedure in Ref. [71] is indeed similar to measuring the energy response to a temperature change: The resulting FDT properties are also found to be of an unusual type [72] in this case. However, the notion of an effective temperature [52] implies that the FDT relations of all observables evolving on the same time scale should be identical. As suggested in Refs. [28,69], an interesting open question is the following: does a measurement in the Tetris model done with a more standard infinitesimal perturbation lead to the same FDT relation? This point deserves a more detailed investigation in this and other glassy models.

The dynamic transition, and the regime (II). We have found a well-defined transition in the phase diagram of Fig. 14. This is in complete agreement with experimental and numerical observations of the existence of a critical value of the drive $\Gamma^\star$, below which glassy effects may be observed. The existence of this dynamical transition provides a very natural context for the interpretation of the numerous non-equilibrium effects encountered in granular matter. Indeed, the transition line in the Fig. 14 links the standard glass transition arising at $T = T_c$, and $\Gamma = 0$ in the glassy model to the dynamical transition arising at $T = 0$ and $\Gamma = \Gamma^\star$ in the driven dynamics of athermal systems. In our opinion, this result gives a nice theoretical support to the analogy between glasses and granular materials, making a deep connection between the two situations.

We wish to emphasize that it was not evident *a priori* that the transition could survive a finite time-dependent driving force. This is one of the main results of this paper, and it has to be compared to the very different effect of shearlike forces. Indeed, an infinitesimal shearlike perturbation is enough to introduce a finite time scale in this model, and aging is hence interrupted [18,21].

The liquid regime (II) is less interesting in the present context, since no slow dynamics is present. Let us stress that the system is still strongly driven, and hence no ''equilibrium'' state, in the sense of statistical mechanics, is reached.

In particular, no effective FDT temperature can be defined: the system is completely athermal. The very existence of an effective temperature relies indeed on the existence of two well-separated time scales, allowing the slow degrees of freedom to thermalize and the susceptibility and correlation parametric curves of Fig. 9(a) are not very useful to describe this non-equilibrium situation.

VI. CONCLUSION: TOWARD A THERMODYNAMICAL DESCRIPTION OF SLOW GRANULAR RHEOLOGY?

The interpretation of FDT violations in terms of an effective temperature T_{EFF} was developed in Ref. [52]. Having a well-defined concept of temperature is a crucial first step in a thermodynamical description of granular materials [73]. It is then important to discuss the possibility of a link with previous thermodynamical concepts in the granular literature.

The notion of a ''granular temperature'' was introduced to extend thermodynamics to strongly perturbed powders [1]. In analogy with the kinetic gas theory, it was assumed that the distribution of the grain velocity v is Maxwellian. Via the equipartition relation, one gets $T \propto \langle v^2 \rangle$. We have been concerned with a weakly perturbed regime, where the dynamics is slow. This hydrodynamic definition is not supposed to be relevant in this case. This is also well known in the field of glasses, where nontrivial effective temperatures are known to exist while the kinetic energy is an observable that very rapidly equilibrates with its environment, leading to a kinetic temperature that coincides with the temperature of the bath. Very recently [74], an attempt to extend the hydrodynamic theory to a regime where the grains are *not* fluidized was proposed, also using the concept of kinetic granular temperature. It would then be very interesting to try to understand the two concepts in a unified way.

More related to ours is the approach of Mehta and co-workers [8], discussed in Sec. I. This phenomenological two-step, two-temperature model finds a nice justification within the scenario emerging from our results. This model was in fact inspired by the illuminating work initiated in the late 1980s by Edwards and his collaborators [38]. The postulated thermodynamic relations in analogy with the usual ''thermal'' thermodynamics, where the volume V plays the role of the internal energy U. In this approach, the entropy is the logarithm of the number of configurations with volume V. The so-called compactivity X is the analog of the temperature, and it is defined as [38]

$$\frac{1}{X} \equiv \frac{\partial S}{\partial V}, \tag{29}$$

still by analogy with the usual definition $T^{-1} \equiv \partial S / \partial U$. The connection between the compactivity X and the FDT temperature T_{EFF} discussed in this paper has already been explored [10,57,58,62,71]. Crucially for our study, *Edwards' definition of the compactivity coincides with the (asymptotic) FDT effective temperature* defined in Eq. (14). This result holds for mean-field models like the one discussed here [62], as well as in the lattice gas model studied in Ref. [57]. However, these studies have been done without an external forc-

ing. It would be very interesting to extend the numerical analysis of Ref. [57] to the same model now driven by an ac force.

We have obtained here that the existence of an effective temperature for the slow decay resists a finite ac force. This supports the conjecture that definitions (14) and (29) may be of fundamental interest for the study of glassy and granular materials. Computing them in realistic models is then a challenge for future research [57,58,62,75]. In this respect, very recent works [76] studying spin models on random graphs may give some insights into the role played by metastable states, which can have an important influence on the dynamics, as we showed in Sec. IV C.

In conclusion, we have found that the study of driven-

glassy systems provides a theoretical framework to understand the slow granular rheology. The existence of a dynamical transition well justifies the use of ''modified glassy models'' to describe granular materials. The existence of an effective temperature for the slow degrees of freedom provides, in particular, a nice theoretical basis to previous ''thermal'' models for granular matter, and to the seminal approach of Edwards.

[1] H. M. Jaeger, S. R. Nagel, and R. P. Behringer, Rev. Mod. Phys. **68**, 1259 (1996); H. M. Jaeger and S. R. Nagel, Science **255**, 1523 (1992); P. G. de Gennes, Rev. Mod. Phys. **71**, S374 (1999).

[2] J. B. Knight, C. G. Fandrich, C. N. Lau, H. M. Jaeger, and S. R. Nagel, Phys. Rev. E **51**, 3957 (1995); E. R. Nowak, J. B. Knight, E. Ben-Naim, H. M. Jaeger, and S. R. Nagel, *ibid.* **57**, 1971 (1998).

[3] M. Nicolas, P. Duru, and O. Pouliquen, Eur. Phys. J. C **3**, 309 (2000).

[4] H. M. Jaeger, C.-H. Liu, and S. R. Nagel, Phys. Rev. Lett. **62**, 40 (1989).

[5] É. Falcon, R. Wunenburger, P. Évesque, S. Fauve, C. Chabot, Y. Garrabos, and Daniel Beysens, Phys. Rev. Lett. **83**, 440 (1999), and references therein.

[6] S. F. Edwards and D. V. Grinev, e-print cond-mat/9905114.

[7] A. J. Liu and S. R. Nagel, Nature (London) **396**, 21 (1998).

[8] A. Mehta, R. J. Needs, and S. Dattagupta, J. Stat. Phys. **68**, 1131 (1992).

[9] A. Mehta and G. C. Barker, J. Phys.: Condens. Matter **12**, 6619 (2000); G. C. Barker and A. Mehta, Phys. Rev. E **47**, 184 (1993); A. Mehta and G. C. Barker, Phys. Rev. Lett. **67**, 394 (1991); G. C. Barker and A. Mehta, Phys. Rev. A **45**, 3435 (1992).

[10] J. Kurchan, e-print cond-mat/9812347; J. Phys.: Condens. Matter **12**, 6611 (2000).

[11] J.-P. Bouchaud, L. F. Cugliandolo, J. Kurchan, and M. Mézard, in *Spin Glasses and Random Fields*, edited by A. P. Young (World Scientific, Singapore, 1998).

[12] L. C. E. Struik, *Physical Aging in Amorphous Polymers and Other Materials* (Elsevier, Houston, 1978); L. Bellon, S. Ciliberto, and C. Laroche, Europhys. Lett. **51**, 551 (2000).

[13] E. Vincent, J. Hammann, M. Ocio, J.-Ph. Bouchaud, and L. F. Cugliandolo, in *Complex Behavior of Glassy Systems*, edited by M. Rubi (Springer-Verlag, Berlin, 1997); P. Nordblad and P. Svendlidh, in *Spin Glasses and Random Fields*, edited by A. P. Young (World Scientific, Singapore, 1998).

[14] R. L. Leheny and S. R. Nagel, Phys. Rev. B **57**, 5154 (1998); T. Grigera and N. Israeloff, Phys. Rev. Lett. **83**, 5038 (1999).

[15] F. Alberici-Kious, J.-Ph. Bouchaud, L. F. Cugliandolo, P. Doussineau, and A. Levelut, Phys. Rev. Lett. **81**, 4987 (1998).

[16] M. Kroon, G. H. Wegdam, and R. Sprick, Phys. Rev. E **54**, 6541 (1996); D. Bonn *et al.*, Europhys. Lett. **45**, 52 (1998); A. Knaebel *et al.*, *ibid.* **52**, 73 (2000); L. Cipelletti *et al.*, Phys. Rev. Lett. **84**, 2275 (2000).

[17] A. J. Bray, Adv. Phys. **43**, 357 (1994).

[18] L. F. Cugliandolo, J. Kurchan, P. Le Doussal, and L. Peliti, Phys. Rev. Lett. **78**, 350 (1997).

[19] A. Onuki, J. Phys. C **9**, 6119 (1997).

[20] R. G. Larson, *The Structure and Rheology of Complex Fluids* (Oxford University Press, New York, 1999).

[21] L. Berthier, J.-L. Barrat, and J. Kurchan, Phys. Rev. E **61**, 5464 (2000).

[22] P. Sollich, Phys. Rev. E **58**, 738 (1998); S. M. Fielding, P. Sollich, and M. E. Cates, J. Rheol. **44**, 323 (2000).

[23] C. Dérec, A. Ajdari, and F. Lequeux, Faraday Discuss. **112**, 195 (1999); Eur. Phys. J. E **4**, 355 (2001).

[24] C. Josserand, A. Tkachenko, D. M. Mueth, and H. M. Jaeger, Phys. Rev. Lett. **85**, 3632 (2000).

[25] G. D'Anna, e-print cond-mat/0006323.

[26] A. Coniglio and H. J. Herrmann, Physica A **225**, 1 (1996); M. Nicodemi, A. Coniglio, and H. J. Herrmann, Phys. Rev. E **55**, 3962 (1997); J. Phys. A **30**, L379 (1997).

[27] M. Nicodemi and A. Coniglio, Phys. Rev. Lett. **82**, 916 (1999); A. Coniglio and M. Nicodemi, Phys. Rev. E **59**, 2812 (1999); J. Phys. C **12**, 6601 (2000).

[28] A. Barrat and V. Loreto, J. Phys. A **33**, 4401 (2000); e-print cond-mat/0006413.

[29] M. Sellitto and J. J. Arenzon, Phys. Rev. E **62**, 7793 (2000).

[30] T. Boutreux and P. G. de Gennes, Physica A **244**, 59 (1997).

[31] A. J. Kolan, E. R. Nowak, and A. V. Tkachenko, Phys. Rev. E **59**, 3094 (1999); J. Talbot, G. Tarjus, and P. Viot, Phys. Rev. E **61**, 5429 (2000); e-print cond-mat/0008183.

[32] S. J. Linz, Phys. Rev. E **54**, 2925 (1996).

[33] D. C. Hong, S. Yue, J. K. Rudra, M. Y. Choi, and Y. W. Kim, Phys. Rev. E **50**, 4123 (1994).

[34] K. L. Gavrilov, Phys. Rev. E **58**, 2107 (1998).

[35] D. A. Head and G. J. Rodgers, J. Phys. A **31**, 107 (1998).

[36] D. A. Head, Phys. Rev. E **62**, 2439 (2000).

[37] S. F. Edwards and D. V. Grinev, Phys. Rev. E **58**, 4758 (1998).

[38] S. F. Edwards, in *Disorder in Condensed Matter Physics* (Ox-

ford Science, New York, 1991); and in *Granular Matter: An Interdisciplinary Approach*, edited by A. Mehta (Springer-Verlag, New York, 1994), and references therein.

[39] J.-L. Barrat and L. Berthier, Phys. Rev. E **63**, 012 503 (2001).

[40] ac perturbations of short duration, typically a few cycles, have been experimentally used to probe the dynamics of glassy materials in, e.g., nonresonant hole-burning experiments [41,42]. A careful study of the dynamics of glassy systems under a permanent ac perturbation is, as far as we know, still lacking.

[41] M. T. Cicerone and M. D. Ediger, J. Chem. Phys. **103**, 5684 (1995); R. Böhmer *et al.*, J. Non-Cryst. Solids **235-237**, I-9 (1998), and references therein.

[42] L. F. Cugliandolo and J. L. Iguain, Phys. Rev. Lett. **85**, 3448 (2000).

[43] T. R. Kirkpatrick and D. Thirumalai, Phys. Rev. B **36**, 5388 (1987).

[44] A. Crisanti and H.-J. Sommers, Z. Phys. B: Condens. Matter **87**, 341 (1992).

[45] J. M. Kosterlitz, D. J. Thouless, and R. C. Jones, Phys. Rev. Lett. **36**, 1217 (1976).

[46] P. Shukla and S. Singh, Phys. Rev. B **23**, 4661 (1981); S. Ciuchi and F. de Pasquale, Nucl. Phys. B **300**, 31 (1988).

[47] L. F. Cugliandolo and D. S. Dean, J. Phys. A **28**, 4213 (1995); W. Zippold, R. Kuehn, and H. Horner, Eur. Phys. J. B **13**, 531 (2000).

[48] L. F. Cugliandolo and D. S. Dean, J. Phys. A **28**, L453 (1995).

[49] M. Mézard and G. Parisi, J. Chem. Phys. **111**, 1076 (1999).

[50] L. F. Cugliandolo and J. Kurchan, Phys. Rev. Lett. **71**, 173 (1993).

[51] B. Derrida, Phys. Rev. B **24**, 2613 (1981); D. J. Gross and M. Mézard, Nucl. Phys. B **240**, 431 (1984).

[52] L. F. Cugliandolo, J. Kurchan, and L. Peliti, Phys. Rev. E **55**, 3898 (1997).

[53] L. F. Cugliandolo and J. Kurchan, J. Phys. A **27**, 5749 (1994).

[54] S. A. Langer and A. J. Liu, Europhys. Lett. **49**, 68 (2000).

[55] P. H. Stillinger and T. A. Weber, Science **255**, 983 (1984).

[56] W. Kob, F. Sciortino, and P. Tartaglia, Europhys. Lett. **49**, 590 (2000); G. Biroli and R. Monasson, *ibid.* **50**, 155 (2000).

[57] A. Barrat, J. Kurchan, V. Loreto, and M. Sellitto, Phys. Rev. Lett. **85**, 5034 (2000); e-print cond-mat/0011492.

[58] A. Coniglio and M. Nicodemi, e-print cond-mat/0010191.

[59] L. F. Cugliandolo, D. S. Dean, and J. Kurchan, Phys. Rev. Lett. **79**, 2168 (1997).

[60] W. Götze, in *Liquids, Freezing and Glass Transition*, edited by J. P. Hansen, D. Levesque, and J. Zinn-Justin, Les Houches 1989 (North-Holland, Amsterdam, 1991); W. Götze and L. Sjögren, Rep. Prog. Phys. **55**, 241 (1992); W. Götze, J. Phys.: Condens. Matter **11**, A1 (1999).

[61] J. Kurchan, G. Parisi, and M. A. Virasoro, J. Phys. I **3**, 1819 (1993); A. Barrat, R. Burioni, and M. Mézard, J. Phys. A **29**, L81 (1996); A. Cavagna, I. Giardina, and G. Parisi, Phys. Rev. B **57**, 11 251 (1998).

[62] R. Monasson, Phys. Rev. Lett. **75**, 2847 (1995); R. Monasson and O. Pouliquen, Physica A **236**, 395 (1997).

[63] A. Cavagna, J. P. Garrahan, and I. Giardina, J. Phys. A **32**, 711 (1999).

[64] E. Kolb and E. Clément, Eur. J. Phys. B **8**, 483 (1999); L. Vanel and É. Clément, *ibid.* **11**, 525 (1999); L. Vanel, thèse de doctorat de l'Université Paris 6 (1999).

[65] For a review, see J.-P. Bouchaud, in *Soft and Fragile Matter, Nonequilibrium, Metastability and Flow*, edited by M. E. Cates and M. R. Evans (Institute of Physics Publishing, Bristol, 2000).

[66] J. P. Sethna, O. Perkovic, and K. A. Dahmen, in *Scale Invariance and Beyond*, edited by B. Dubrulle, F. Graner, and D. Sornette (Springer, Berlin, 1997), and references therein.

[67] L. Berthier, J.-L. Barrat, and J. Kurchan, Phys. Rev. E **63**, 016 105 (2001).

[68] L. Bellon, S. Ciliberto, and C. Laroche, Europhys. Lett. **53**, 511 (2001).

[69] M. Sellitto, e-print cond-mat/0012273.

[70] H. Makse (unpublished).

[71] M. Nicodemi, Phys. Rev. Lett. **82**, 3734 (1999).

[72] S. M. Fielding and P. Sollich (unpublished).

[73] Also see, in the context of glassy systems, T. M. Nieuwenhuizen, Phys. Rev. E **61**, 267 (2000), and references therein; S. Franz and M. A. Virasoro, J. Phys. A **33**, 891 (2000).

[74] W. Losert, L. Bocquet, T. C. Lubensky, and J. P. Gollub, Phys. Rev. Lett. **85**, 1428 (2000); L. Bocquet, W. Losert, T. C. Lubensky, and J. P. Gollub, e-print cond-mat/0012356.

[75] G. Biroli and J. Kurchan, e-print cond-mat/0005499.

[76] J. Berg and A. Mehta, e-print cond-mat/0012416; D. S. Dean and A. Lefevre, e-print cond-mat/0101166.